J Therm Anal Calorim (2017) 127:789–797
DOI 10.1007/s10973-016-5413-y

Kinetic analysis of poly(ethylene oxide)/lithium montmorillonite nanocomposites

Matko Erceg[1] · Irena Krešić[1] · Miće Jakić[1] · Branka Andričić[1]

Received: 29 October 2015 / Accepted: 23 March 2016 / Published online: 9 April 2016

Abstract Poly(ethylene oxide)/lithium montmorillonite (PEO/LiMMT) nanocomposites were prepared by melt intercalation method. The degradation of PEO/LiMMT nanocomposites was performed by non-isothermal thermogravimetry in nitrogen atmosphere at four heating rates (2.5, 5, 10 and 20 °C min^{-1}). The obtained data were used for the kinetic analysis of the degradation process. Kinetic analysis was performed using the isoconversional Friedman method in combination with the multivariate nonlinear regression method. Kinetic analysis revealed the complexity of the thermal degradation process for both pure PEO and all PEO/LiMMT nanocomposites. The contribution of the each individual degradation stage was determined, and each of them was independently analyzed. Kinetic parameters (activation energy, pre-exponential factor and kinetic model) were also calculated for each degradation stage of all investigated samples.

Keywords Kinetic analysis · Multivariate nonlinear regression method · Poly(ethylene oxide) · Lithium montmorillonite

Introduction

Poly(ethylene oxide) (PEO)-based solid polymer electrolytes (SPE) are becoming increasingly important for the development of rechargeable lithium polymer batteries due to their enhanced safety, flexibility and manufacturability. Consequently, PEO-based SPEs are among the most studied polymer ionic conductors [1–5]. However, the high crystallinity of PEO limits the lithium ion transport resulting in a poor ionic conductivity of PEO-based electrolytes at ambient temperature. In order to reduce crystallinity and increase its ionic conductivity, nanocomposites of PEO with lithium montmorillonite (LiMMT) have been prepared and characterized, as presented in our earlier work [6]. Obtained results have shown the significant increase in ionic conductivity at ambient temperature with the addition of LiMMT. Furthermore, results obtained from the non-isothermal thermogravimetric (TG) analysis have shown that addition of LiMMT lowers the thermal stability of PEO and influences the mechanism of PEO thermal degradation.

The experimental data obtained by the non-isothermal thermogravimetry are very often used for kinetic analysis. Kinetic analysis aims to reveal the mechanism of thermally stimulated process and to calculate kinetic parameters of the investigated process, i.e., the activation energy (E), the pre-exponential factor (A) and kinetic model ($f(\alpha)$), the so-called kinetic triplet. Kinetic analysis of the non-isothermal degradation of PEO has already been studied and reported in the literature. Pielichowski and Flejtuch [7] have investigated thermal degradation of PEO and by applying the nonlinear regression method, and F test concluded that three-dimensional phase boundary reaction (R3) gave the best fit of the non-isothermal degradation of PEO. Calahorra et al. [8] have obtained E value of 129 kJ mol^{-1} assuming the first-order reaction (F1) kinetic model for PEO of $M_w = 365{,}000$. Barbadillo et al. [9] have found that nth-order reaction models are not applicable for kinetic description of the non-isothermal degradation of PEOs of M_w from 1500 to 3000. In our earlier work [10], we have concluded that the non-isothermal degradation of PEO of different molecular masses in the conversion range

✉ Matko Erceg
merceg@ktf-split.hr

[1] Faculty of Chemistry and Technology, University of Split, Ruđera Boškovića 35, 21000 Split, Croatia

0.10–0.90 occurs through a mechanism like those represented by Avrami–Erofeev equation (*An*). Finally, in our latest work on the non-thermal degradation of poly(vinyl chloride) and PEO blends [11], the kinetic analysis indicated complex degradation mechanism of PEO ($M_w = 100{,}000$) where Avrami–Erofeev (*An*) kinetic model is defined as the main kinetic model for characterization of the degradation process.

To our knowledge, besides our recently published paper [6] in which complexity of the non-isothermal degradation of PEO/LiMMT nanocomposites is only noticed but not analyzed in details, there are no published papers concerning the kinetic analysis of the non-isothermal degradation of PEO/LiMMT nanocomposites. Therefore, the purpose of this article is to reveal the complexity of the non-isothermal degradation of PEO/LiMMT nanocomposites and to calculate corresponding kinetic parameters in a whole conversion range. For this purpose, isoconversional Friedman (FR) [12] method in combination with the multivariate nonlinear regression method was used.

Experimental

PEO powder with viscometric average molecular mass of 300,000 was purchased from Sigma-Aldrich. LiMMT was prepared by ion exchange from natural montmorillonite (Cloisite®Na+, Southern Clay Products Inc., USA) and lithium chloride (Kemika, Croatia). Ion exchange has been carried out by suspending 15.0 g of Cloisite®Na^+ in 400 cm^3 of 1.0 mol dm^{-3} LiCl solution in de-ionized water. The suspension was stirred on a magnetic stirrer for 48 h at 40 °C. The mixture was then centrifuged at 5000 rpm until a clear separation was obtained and the supernatant was decanted. A series of washings with de-ionized water and again centrifugation were performed until the chloride ions were completely removed (tested using $AgNO_3$ solution). The obtained residue is LiMMT. LiMMT was then dried in an oven for 5 h at 120 °C and then in a vacuum oven for 48 h at 100 °C. PEO/LiMMT nanocomposites with compositions 100/0 (pure PEO), 95/5, 90/10, 85/15, 80/20 and 75/25 by mass were prepared by melt intercalation. Powders of PEO and LiMMT in the required mass ratios were manually mixed for 10 min using an agate mortar and shaped into pellets by a hydraulic press and a load of 5 tons. The obtained samples were 13 mm in diameter, with a thickness of 0.7–0.8 mm. Melt intercalation was performed at 90 °C for 8 h in a vacuum oven.

The experimental data for the kinetic analysis were obtained by non-isothermal thermogravimetry (TG). The thermal degradation of PEO/LiMMT samples (sample mass 9.3 ± 0.5 mg, standard platinum sample pan) was performed in the temperature range 50–500 °C at the heating rates 2.5, 5, 10 and 20 °C min^{-1} using a Perkin-Elmer Pyris 1 thermobalance. The nitrogen flow rate was 30 cm^3 min^{-1}. Before operating, the system was stabilized for 1 h at initial temperature and nitrogen flow.

Kinetic analysis

Kinetic analysis of the solid-state reactions is based on Eq. (1):

$$\frac{d\alpha}{dt} \cong \beta \frac{d\alpha}{dT} = A \times \exp\left(-\frac{E}{RT}\right) \times f(\alpha) \quad (1)$$

where α is the degree of conversion, β is the linear heating rate (°C min^{-1}), T is the absolute temperature (K), R is the general gas constant (J mol^{-1} K^{-1}) and t is the time (min). Kinetic analysis should begin with the investigation of the process complexity by determining the dependence of E on α by isoconversional methods [13–17]. Dependence of E on α is taken as a reliable criterion of the process complexity, and isoconversional methods are considered as the most reliable methods for the calculation of E and E versus α dependence of thermally activated reactions. If E is roughly constant over the entire conversion range and if no shoulders are observed in the reaction rate curve, it is likely that a process is dominated by a single reaction step and can be adequately described by a single-step model [13]. If E changes with α, the process is complex and the shape of the E versus α curve may indicate the possible reaction mechanism [13–15, 18]. Therefore, E values and E versus α dependence can be calculated directly from experimental data by using an isoconversional Friedman method without knowledge or assumption of kinetic model (model-free method). On the other hand, Friedman method does not give any information about A and $f(\alpha)$.

To overcome this problem, kinetic analysis in this work was performed using model fitting multivariate nonlinear regression method incorporated in Netzsch Thermokinetic 3.1 software. This method is based on fitting of either single- or multi-step models to experimental data. A series of reaction model types is listed in Table 1. This list contains classic models for homogeneous reactions and for typical solid reactions. In comparison with known reaction model types [13], the list is extended with the combined autocatalytic model types C1 and Cn [19]. Fitting of selected model(s) is commonly accomplished by minimizing the difference between the measured and calculated data. In order to find the best kinetic model, a method of least squares and F test method are used.

Isoconversional Friedman method

Isoconversional Friedman (FR) method enables determination of E directly from experimental α–T data

Table 1 Reaction model types and corresponding reaction equations $de/dt = -A\ \exp(E/RT)f(e,p)$: e is start concentration of the reactant ($e = 1 - \alpha$), and p is concentration of the final product ($p = \alpha$) [19]

Code	$f(e,p)$	Reaction type
F1	e	First-order reaction
F2	e^2	Second-order reaction
Fn	e^n	*n*th-Order reaction
R2	$2e^{1/2}$	Two-dimensional phase boundary reaction
R3	$3e^{2/3}$	Three-dimensional phase boundary reaction
D1	$0.5/(1 - e)$	One-dimensional diffusion
D2	$-1/\ln(e)$	Two-dimensional diffusion
D3	$1.5e^{1/3}/(e^{-1/3} - 1)$	Three-dimensional diffusion (Jander's type)
D4	$1.5/(e^{-1/3} - 1)$	Three-dimensional diffusion (Ginstling–Brounstein type)
B1	ep	Simple Prout–Tompkins equation
Bna	$e^n p^a$	Expanded Prout–Tompkins equation (*na*)
C1-X	$e\ (1 + KcatX)$	First-order reaction with autocatalysis through the reactants, X X = a product in the complex model, frequently $X = p$
Cn-X	$e^n\ (1 + KcatX)$	*n*th-Order reaction with autocatalysis through the reactants, X
A2	$2e\ (-\ln(e))^{1/2}$	Two-dimensional nucleation
A3	$3e\ (-\ln(e))^{2/3}$	Three-dimensional nucleation
An	$ne\ (-\ln(e))^{(n-1)/n}$	*n*-Dimensional nucleation/nucleus growth according to Avrami–Erofeev

($\alpha = (m_0 - m)/(m_0 - m_f)$, where m_0, m and m_f refer to the initial, actual and residual mass of the sample obtained at several heating rates without the knowledge of $f(\alpha)$. FR method is a linear differential method based on Eq. (2):

$$\ln\left[\beta\frac{d\alpha}{dT}\right] = \ln A + \ln f(\alpha) - \frac{E}{RT} \quad (2)$$

Plots $\ln[\beta(d\alpha/dT)]$ versus $1/T$ obtained for each selected $\alpha = \text{const.}$ from α–T curves recorded at several heating rates should be straight lines whose slopes allow calculation of E by means of FR method.

Results and discussion

The experimental data for the kinetic analysis were obtained from the corresponding non-isothermal thermogravimetric (TG) measurements. As the representative experimental data, the TG curves of PEO, PEO/LiMMT 90/10 and PEO/LiMMT 80/20 are presented in Fig. 1. The experimental data for other samples are used for the kinetic analysis, and obtained results are shown in corresponding tables and figures.

For each selected $\alpha = \text{const.}$, the corresponding plots according to Eq. (2) had been obtained, and from their slopes, E values are calculated. The dependences of E on α evaluated by means of FR method in a whole conversion range are shown in Fig. 2. It is obvious from Fig. 2 that if the whole conversion range is observed, E depends on α for all investigated samples, which indicates the complex (multi-step) degradation mechanism. Consequently, since E depends on α, the whole degradation process cannot be described adequately by a single reaction model and a single pair of Arrhenius parameters. In this case, it is advised to resort to a multi-step kinetic analysis that would yield an individual reaction model and a pair of Arrhenius parameters for each of the reaction steps. Such an analysis can be accomplished by using the model fitting multivariate nonlinear regression method [13–15, 20].

Inspection of Fig. 2 clearly shows that there are also conversion regions for all investigated samples where E can be considered almost constant. This conversion range where E does not depend on α is the largest for pure PEO and it is getting smaller with the increasing addition of LiMMT. This is obvious indication that addition of LiMMT changes the degradation mechanism of PEO and this article aims to reveal and quantify that change.

In our previous study of the non-isothermal degradation of PEO [10], it has been concluded that degradation takes place in one main stage in a conversion range 0.10–0.90 since in that conversion range E did not significantly depend on α. Kinetic analysis has been performed by combining the isoconversional (Friedman, Flynn–Wall–Ozawa and Kissinger–Akahira–Sunose) and invariant kinetic parameters (IKP) methods. Avrami–Erofeev kinetic models have been found as the most probable ones for the kinetic description of the non-isothermal degradation of PEO [10]. But, IKP method is limited to the conversion range where E does not change significantly with α, and therefore, the whole conversion range could not be

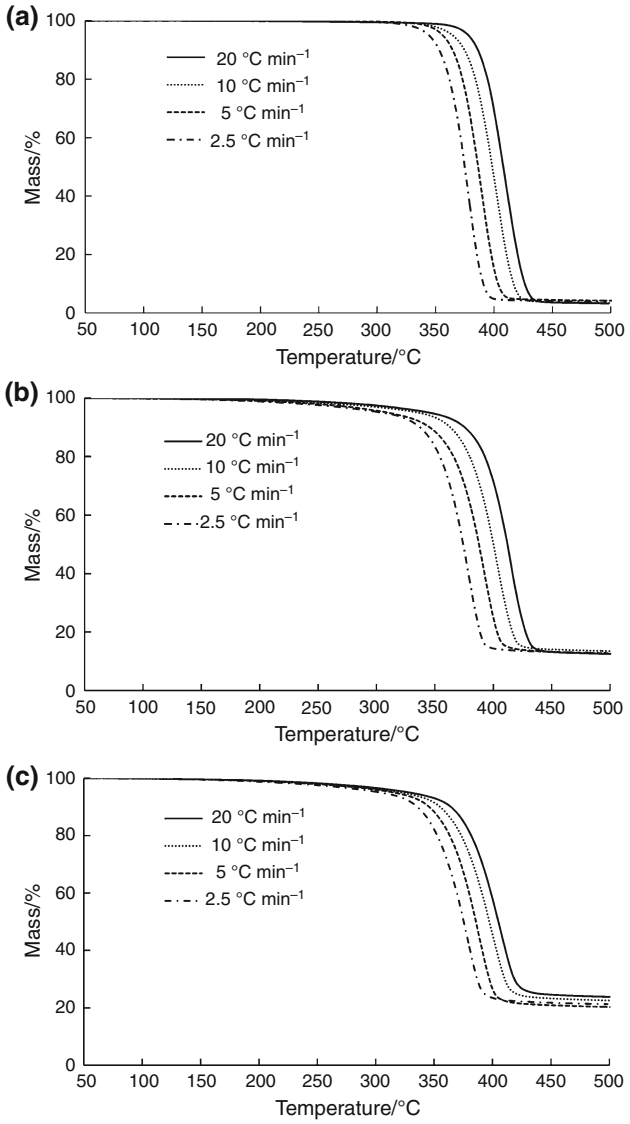

Fig. 1 Thermogravimetric (TG) curves for PEO (**a**), PEO/LiMMT 90/10 (**b**) and PEO/LiMMT 80/20 (**c**) nanocomposites

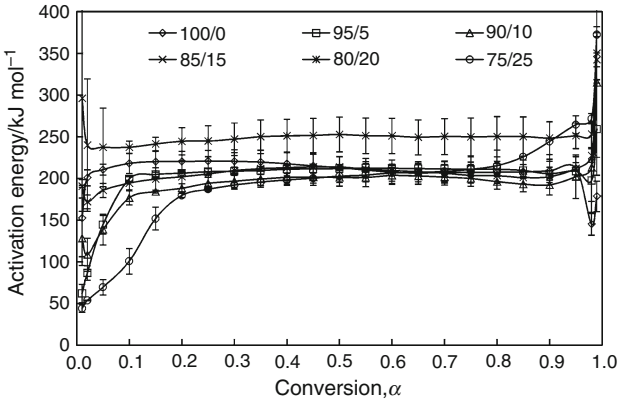

Fig. 2 Dependence of E on α determined by Friedman method in a whole conversion range for thermal degradation of all analyzed samples

investigated. Mathematical tools available for the purpose of this work (model fitting multivariate nonlinear regression method incorporated in Netzsch Thermokinetic 3.1 software) enable kinetic analysis in the whole conversion range. Upon a detailed examination of apparent activation energy of PEO non-isothermal degradation calculated by the FR method (Fig. 2), three conversion areas with different E values can be observed. This means that from the kinetical point of view PEO degradation can be adequately described by three individual reaction models and corresponding pairs of Arrhenius parameters. These three stages of the PEO degradation can also be visualized by checking derivative thermogravimetric curves (DTG curves). To justify the occurrence of multiple degradation stages, a deconvolution procedure described in details by Perejón et al. [21] was performed. MagicPlot Pro computer program and different fitting functions (Gaussian and Lorentzian) were used for the deconvolution process. The fitting results for PEO are given in Fig. 3a. Figure 3a shows experimental DTG curves (circles), fitted (dotted) and cumulative (solid lines) curves at 5 °C min^{-1}, respectively. Cumulative curves are obtained by summation of individual fitting curves. It is obvious from Fig. 3a that DTG curve of pure PEO is asymmetrical and can be well fitted with three functions, supporting the above-mentioned conclusion that its thermal degradation can be adequately described by three individual reaction steps. The residual mass of pure PEO does not depend on the heating rate (Fig. 1a) which eliminates the possibility of the branched reaction path. Namely, the dependence of residual mass on the heating rate is a serious indication that the branched reaction path exists and unbranched reaction path is present if the remaining mass does not depend on the heating rate [22].

As much as PEO/LiMMT nanocomposites are concerned, there are no data in the literature on their kinetic analysis. In our earlier work [6], isoconversional analysis (Friedman method) has been performed and it was concluded that the addition of LiMMT made thermal degradation of PEO more complex. Detailed examination of apparent activation energy of PEO/LiMMT nanocomposites calculated by the FR method (Fig. 2) also indicates existence of conversion areas with different E values. The occurrence of multiple degradation stages of the PVC/LiMMT samples was also confirmed by deconvolution of their DTG curves. The fitting results for two specific selected samples (90/10 and 80/20) are given in Fig. 3b, c, respectively. It is obvious from Fig. 3b that DTG curve of PEO/LiMMT 90/10 can be well fitted with four functions, while DTG curve of PEO/LiMMT 80/20 can be well fitted

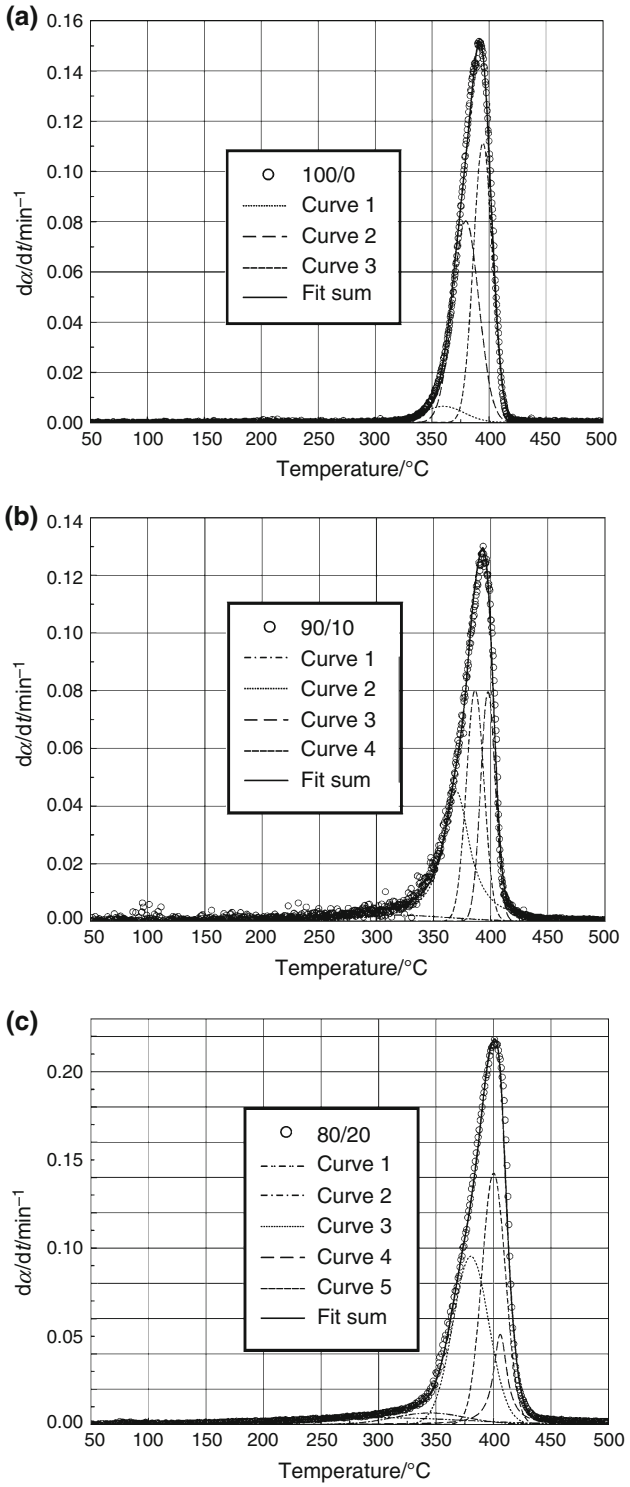

Fig. 3 Overlay of experimental DTG curves (*circles*) at 5 °C min^{-1}, fitted (*dotted*) and cumulative (*solid lines*) curves for PEO (**a**), PEO/LiMMT 90/10 (**b**) and PEO/LiMMT 80/20 (**c**) nanocomposites

with five functions. The residual mass of PEO/LiMMT 90/10 nanocomposites does not depend on the heating rate (Fig. 1b), and therefore, branching reaction path cannot be expected. The residual mass of PEO/LiMMT 80/20 (Fig. 1c) depends on the heating rate which is an indication that the branched reaction path exists. All other analyzed PEO/LiMMT nanocomposites show behavior similar to sample 90/10, i.e., degradation in four stages without branching. It should be emphasized that the number of steps is determined by increasing it consecutively until the introduction of a new step did not result in statistically significant improvement of the fit, as suggested by Vyazovkin [23].

In order to find the most probable kinetic model and calculate kinetic parameters of thermal degradation of PEO and PEO/LiMMT nanocomposites, the multivariate nonlinear regression was employed. The analysis was based on the values of the activation energy as well as on the shape and slope of experimental points and isoconversional lines from Friedman plots. In order to ease the setup of the model, one firstly needs to answer the question whether the remaining mass of the sample depends on the heating rate. It is also important to analyze the experimental points at the start of the reaction ($\alpha = 0.02 - 0.10$) and compare them with Friedman analysis (Fig. 4). If experimental points show a lower slope than the isoconversional Friedman lines, this is a certain indication of the presence of diffusion reaction [22]. Applying statistical criteria, F test and correlation coefficient and especially the similarity of obtained E values with those calculated by FR method made it possible to find the best fit of $f(\alpha)$ functions that reasonably describe kinetic scheme of PEO/LiMMT non-isothermal degradation.

Table 2 shows apparent activation energy values obtained by the FR method for each degradation stage. The results of calculations for the most probable kinetic models on the basis of F test and correlation coefficient are given in Table 3. Finally, in Fig. 5 the comparison of the experimental data (lines) and data calculated from multivariate nonlinear regression for the pure PEO, PEO/LiMMT 90/10 and PEO/LiMMT 80/20 nanocomposites is shown.

As explained earlier, since the activation energy, calculated by Friedman method, depends on the conversion (Fig. 2a) and the remaining mass of PEO does not depend on the heating rate (Fig. 1a), it is reasonable to conclude that the non-isothermal degradation of PEO occurs through multi-step unbranched reaction, in this case through consecutive reactions. The best fit between the experimental data and the assumed kinetic models was also obtained for the three-stage degradation mechanism $A \xrightarrow{1} B \xrightarrow{2} C \xrightarrow{3} D$, which was confirmed by the high correlation coefficient, r^2 of 0.99996. Since the experimental starting points coincide with Friedman isoconversional lines (Fig. 3a), F1, F2, R2 and R3 kinetic models are suggested as possible ones [22]. Indeed, performed

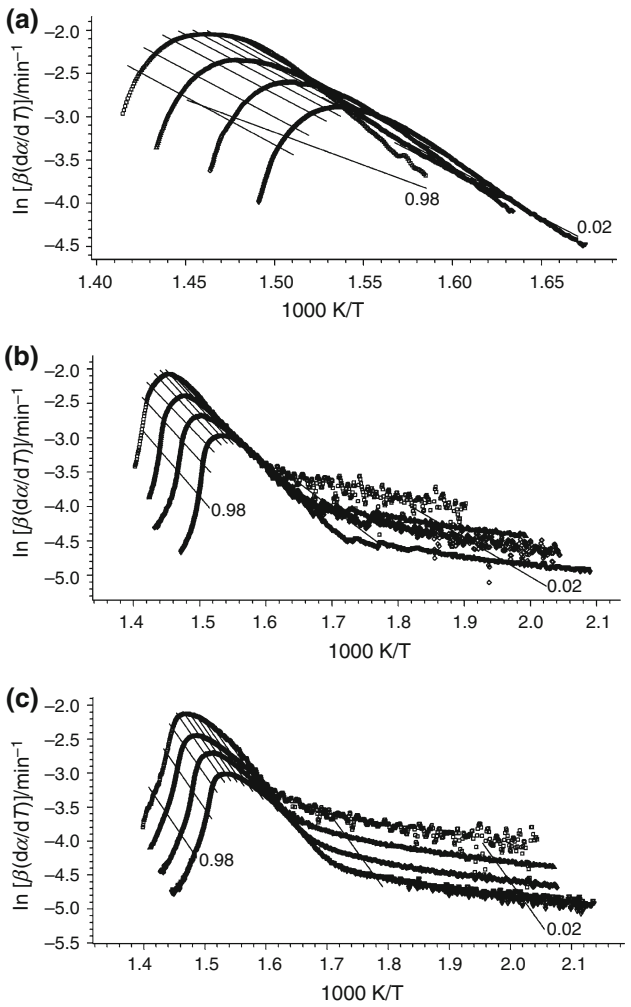

Fig. 4 Friedman plots for the thermal degradation for PEO (**a**), PEO/LiMMT 90/10 (**b**) and PEO/LiMMT 80/20 (**c**) nanocomposites

kinetic analysis shows that all these four kinetic models are statistically equally probable. Since there is no reason for a special reaction type, the universal *n*th-order (*Fn*) kinetic model is selected as the kinetic model for the start of reaction. According to FR analysis, the apparent activation energy of the first stage ($\alpha = 0.00$–0.05) of thermal degradation of PEO (Fig. 2; Table 2) amounts in the range 152.4–203.1 kJ mol^{-1}. The activation energy obtained by the multivariate nonlinear regression corresponding to *Fn* model amounts 199.0 kJ mol^{-1} (Table 3) and is in accordance with the values obtained by FR methods. The second stage ($\alpha = 0.05$–0.85) and third stage ($\alpha = 0.85$–1.00) of thermal degradation of PEO were described by two Avrami–Erofeev reaction types (*An*) (Table 3). These results support our earlier conclusions that *An* is the best kinetic model for description of the thermal degradation of PEO [10]. It is important to notice that the sensitivity of the applied kinetic software revealed that in practically the same conversion range as in our earlier investigation [10], two *An* models can be observed instead of one. But, it is the same kinetic model (*An*) with somewhat different kinetic parameters and we are inclined to state that this is in an agreement with both our [10] and Madorsky and Strauss [24] investigation who have established that after initiation, PEO decomposes in one main stage by random scission of the chain links without chain-end-initiated depolymerization. The activation energies of 214.9 kJ mol^{-1} and 187.3 kJ mol^{-1} obtained by the multivariate nonlinear regression for the second and third stages (Table 3) are in a very good accordance with the values obtained by FR methods (Table 2) which is a very important indication of correctness of kinetic analysis. Finally, Fig. 5a shows that calculated values are able to describe the experimental data (lines) of the non-isothermal degradation of PEO with very high precision.

The best fit between the experimental data and the assumed kinetic models for PEO/LiMMT 95/5, 90/10, 85/15 and 75/25 nanocomposites was obtained for the four-stage degradation mechanism with unbranched,

Table 2 The range of apparent activation energy values of thermal degradation of PEO/LiMMT nanocomposites obtained by Friedman method

Stage of reaction	Parameter	PEO/LiMMT					
		100/0	95/5	90/10	85/15	80/20	75/25
Stage I	E_1/kJ mol^{-1}	152.4–203.1	62.0–86.6	103.0–138.8	171.0–185.6	237.3–295.8	44.1–69.5
	Conversion range, α	0.00–0.05	0.00–0.05	0.00–0.05	0.00–0.05	0.00–0.02	0.00–0.10
Stage II	E_2/kJ mol^{-1}	210.5–220.6	144.5–199.4	140.0–188.3	186.0–199.2	235.0–241.3	100.7–192.1
	Conversion range, α	0.05–0.85	0.05–0.10	0.05–0.20	0.05–0.10	0.02–0.05	0.10–0.20
Stage III	E_3/kJ mol^{-1}	145.0–212.1	204.7–213.0	194.1–203.5	202.0–213.7	244.5–250.3	195.7–215.2
	Conversion range, α	0.85–1.00	0.10–0.75	0.20–0.60	0.10–0.95	0.05–0.65	0.20–0.90
Stage IV	E_4/kJ mol^{-1}	–	197.3–259.2	192.2–315.2	211.8–342.2	249.8–270.0	225.8–372.3
	Conversion range, α	–	0.75–1.00	0.60–1.00	0.95–1.00	0.65–0.90	0.90–1.00
Stage V	E_5/kJ mol^{-1}	–	–	–	–	251.1–350.2	–
	Conversion range, α	–	–	–	–	0.90–1.00	–

Table 3 The most probable kinetic models of thermal degradation of PEO/LiMMT nanocomposites according to *F* test and correlation coefficient obtained by using multivariate nonlinear regression method

Stage of reaction	Parameter	Sample					
		100/0	95/5	90/10	85/15	80/20	75/25
Stage I	E_1/kJ mol^{-1}	199.0	77.6	104.1	171.5	246.8	66.1
	log A_1	17.6	6.3	6.4	17.0	25.6	2.7
	n	2.8	–	–	–	–	–
	Model	Fn	D3	D3	D3	D3	D3
Stage II	E_2/kJ mol^{-1}	214.0	144.4	169.2	190.9	235.6	120.9
	log A_2	14.6	12.4	11.4	14.2	19.0	8.0
	n	1.3	0.7	0.8	0.3	–	1.2
	Model	An	Fn	Fn	An	D3	An
Stage III	E_3/kJ mol^{-1}	187.3	212.9	201.4	205.3	248.1	214.8
	log A_3	20.9	17.3	13.5	13.9	17.6	15.2
	n	0.2	1.4	1.5	0.7	0.8	1.1
	Model	An	An	An	Fn	An	An
Stage IV	E_4/kJ mol^{-1}	–	222.2	201.1	235.7	269.7	360.0
	log A_4	–	21.7	21.2	16.2	20.3	27.9
	n	–	3.8	3.8	0.3	3.9	3.6
	Model	–	Fn	Fn	Fn	Fn	Fn
Stage V	E_5/kJ mol^{-1}	–	–	–	–	253.3	–
	log A_5	–	–	–	–	14.4	–
	n	–	–	–	–	0.4	–
	Model	–	–	–	–	Fn	–
Correlation coefficient, r^2		0.99992	0.99996	0.99991	0.99992	0.99989	0.99997

consecutive reaction $A \xrightarrow{1} B \xrightarrow{2} C \xrightarrow{3} D \xrightarrow{4} E$ (Table 3). The best fit for PEO/LiMMT 80/20 was obtained for the five-stage degradation mechanisms with branching reaction $A \xrightarrow{1} B \xrightarrow{2} C \xrightarrow{3} D \begin{array}{l} \xrightarrow{4} E \\ \xrightarrow[5]{} F \end{array}$ (Table 3). This is in accordance with the earlier conclusion made on the basis of deconvolution procedure of these samples, as shown in Fig. 3b, c.

Correlation coefficients for all degradation mechanisms are very high and all above 0.9998. Since the experimental starting points have a lower slope than Friedman isoconversional lines (Fig. 3b, c), it is a certain indication of diffusion process [22]. Our calculations show that kinetic model for the start of degradation of all PEO/LiMMT nanocomposites is three-dimensional diffusion (Jander's type) (D3) (Table 3). It is well known that silicate layers of nanoclays act as a mass barrier to volatile products generated during thermal decomposition of polymers [25, 26]. They are impermeable for them and therefore increase the diffusion pathway of volatile products which makes the diffusion rate controlling process at these early stages of degradation. The diffusion is the rate controlling process up to $\alpha = 0.05$ for all samples except the sample with the highest addition of LiMMT (PEO/LiMMT 75/25) where diffusion is the rate controlling up to $\alpha = 0.10$. LiMMT delays chain scission of PEO described with *An* kinetic model to higher conversions compared to pure PEO (Table 3). It is important to note that sample 80/20 has two D3 stages which take place up to conversion of $\alpha = 0.05$. They are recognized by the computational procedure as two stages since they have somewhat different kinetic parameters (E and ln A). But, if they are considered as one stage, for reasons discussed earlier for pure PEO, then thermal degradation of all PEO/LiMMT nanocomposites could practically be described with four-stage process.

In our opinion, it would be too complicated and maybe counterproductive to describe each individual sample and its degradation steps. Therefore, we can summarize that all other stages of degradation for all PEO/LiMMT nanocomposites can be described with either *An* or *Fn* kinetic model (Table 3). These results prove that the addition of LiMMT really influences the thermal degradation and kinetics of PEO. In all PEO/LiMMT nanocomposites except PEO/LiMMT 85/15, *An* remains the main kinetic model for characterization of the degradation process, while *Fn* occurs

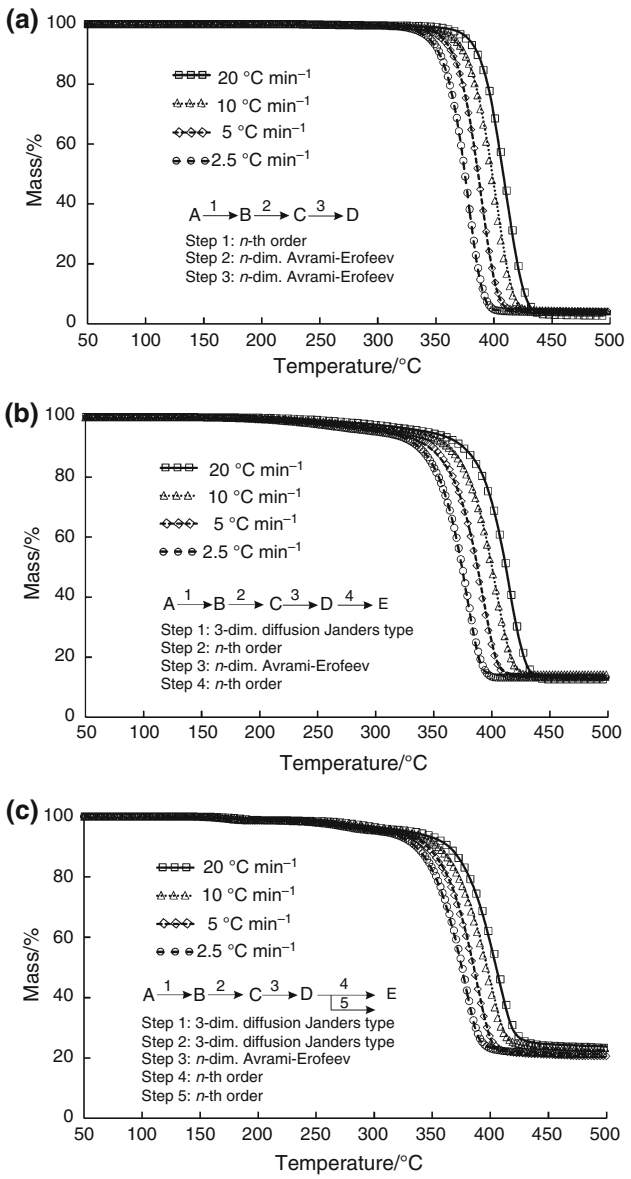

Fig. 5 Comparison of experimental data (*points*) and best-fitted kinetic models (*solid lines*) calculated from multivariate nonlinear regression method for PEO (**a**), PEO/LiMMT 90/10 (**b**) and PEO/LiMMT 80/20 (**c**) nanocomposites

either at the beginning or at the end of degradation process. The kinetic analysis has also shown that the presence of LiMMT as nanofiller lowers the initial activation energy of the PEO degradation (except PEO/LiMMT 85/15) and consequently lowers the onset temperature of degradation as observed in our earlier work [6]. The nanofiller barrier also causes increased charring, which in turn causes higher activation energies at the final stages of degradation of PEO/LiMMT nanocomposites compared to pure PEO.

Figure 5b, c shows the comparison of the experimental data (lines) and calculated data for PEO/LiMMT 90/10 and PEO/LiMMT 80/20 nanocomposites, respectively. Calculated values describe the experimental data (lines) with very high precision.

The kinetic models for the description of the thermal degradation of PEO and PEO/LiMMT nanocomposites presented in this work are selected as the most probable ones on the basis of F test and correlation coefficient, as suggested mutually complement statistical criteria. It is very important to emphasize that calculated E values for calculated kinetic models (Table 3) are in very good agreement with values obtained by isoconversional kinetic models (Table 2). This criterion of similarity with isoconversional E values is crucial for selection of correct kinetic models. Namely, almost all kinetic models can be forced to fit experimental data with a very high correlation coefficient, but only in case of 'true' kinetic model E values similar to those obtained with isoconversional methods will be obtained. In other cases, fitting will be made on the expenses of E and ln A deviation from the real values.

Conclusions

The isoconversional Friedman method in combination with the multivariate nonlinear regression method is employed in order to find the most probable kinetic models of thermal degradation of PEO and PEO/LiMMT nanocomposites. The kinetic analysis indicates three-stage degradation mechanism with consecutive reactions for pure PEO and four-stage degradation mechanism with consecutive reactions for PEO/LiMMT nanocomposites. Exception of this pattern is PEO/LiMMT 80/20 sample which shows five-stage degradation mechanism with a branched reaction path. Kinetic analysis shows that first stage of the non-isothermal degradation of PEO can be well described with nth-order (Fn) kinetic model, followed by two Avrami–Erofeev (An) kinetic models with different kinetic parameters. The addition of LiMMT influences thermal degradation of PEO. The diffusion (D3) is the rate controlling process at the beginning of degradation for all PEO/LiMMT nanocomposites where its influence increases with increasing amounts of LiMMT. An remains the main kinetic model for characterization of the degradation process, while Fn occurs either at the beginning or at the end of degradation process in PEO/LiMMT nanocomposites. Correspondence of activation energies calculated by model fitting multivariate nonlinear regression method with those calculated by the isoconversional Friedman method together with statistical F test and correlation coefficient verified the validity of calculated kinetic models.

References

1. Manoratne CH, Rajapakse RMG, Dissanayake MAKL. Ionic conductivity of poly(ethylene oxide) (PEO)-montmorillonite nanocomposites prepared by intercalation from aqueous medium. Int J Electrochem Sci. 2006;1:32–46.
2. Liao C-S, Ye W-B. Enhanced ionic conductivity in poly(ethylene oxide)/layered double hydroxide nanocomposites electrolytes. J Polym Res. 2003;10:241–6.
3. Sandí G, Carrado KA, Joachin H, Lu W, Prakash J. Polymer nanocomposites for lithium battery applications. J Power Sources. 2003;119–121:492–6.
4. Chen H-W, Chang F-C. The novel polymer electrolyte nanocomposite composed of poly(ethylene oxide), lithium triflate and mineral clay. Polymer. 2001;42:9763–9.
5. Quartatone E, Mustarelli P, Magistris A. PEO-based composite polymer electrolytes. Solid State Ion. 1998;110:1–14.
6. Erceg M, Jozić D, Banovac I, Perinović S, Bernstorff S. Preparation and characterization of melt intercalatedpoly(ethylene oxide)/lithium montmorillonite nanocomposites. Thermochim Acta. 2014;579:86–92.
7. Pielichowski K, Flejtuch K. Non-oxidative thermal degradation of poly(ethylene oxide): kinetic and thermoanalytical study. J. Anal. Appl. Pyrolysis. 2005;73:131–8.
8. Calahorra E, Cortezar M, Guzman GM. Thermal decomposition of poly(ethylene oxide), poly(methyl methacrylate) and their mixtures by thermogravimetric method. J Polym Sci C. 1985;23:257–60.
9. Barbadillo F, Mier JL, Artiaga R, Losada R, García L. Kinetics analysis of the thermal decomposition of polyethylene glycols under inert gas. In: Proceedings of the eight European Symposium on Thermal Analysis and Calorimetry. Barcelona; 2002. p. 75.
10. Vrandečić NS, Erceg M, Jakić M, Klarić I. Kinetic analysis of thermal degradation of poly(ethylene glycol) and poly(ethylene oxide)s of different molecular weight. Thermochim Acta. 2010;498:71–80.
11. Jakić M, Vrandečić NS, Erceg M. Kinetic analysis of the non-isothermal degradation of poly(vinyl chloride)/poly(ethylene oxide) blends. J Therm Anal Calorim. 2016;123:1513–22.
12. Friedman HL. Kinetic of thermal degradation of char-forming plastics from thermogravimetry. Application to a phenolic resin. J Polym Sci C. 1963;6:183–95.
13. Vyazovkin S, Burnham AK, Criado JM, Pérez-Maqueda LA, Popescu C, Sbirrazzuoli N. ICTAC Kinetics Committee recommendations for performing kinetic computations on thermal analysis data. Thermochim Acta. 2011;520:1–19.
14. Vyazovkin S, Sbirrazzuoli N. Isoconversional kinetic analysis of thermally stimulated processes in polymers. Macromol Rapid Commun. 2006;27:1515–32.
15. Vyazovkin S, Chrissafis K, Di Lorenzo ML, Koga N, Pijolat M, Roduit B, Sbirrazzuoli N, Suñol JJ. ICTAC Kinetics Committee recommendations for collecting experimental thermal analysis data for kinetic computations. Thermochim Acta. 2014;590:1–23.
16. Farjas J, Roura P. Isoconversional analysis of solid state transformations. J Therm Anal Calorim. 2011;105:757–66.
17. Sovizi MR, Fakhrpour H, Bagheri S, Bardajee GR. Non-isothermal dehydration kinetic study of a new swollen biopolymer silver nanocomposite hydrogel. J Therm Anal Calorim. 2015;121:1383–91.
18. Fakhrpour G, Bagheri S, Golriz M, Shekari M, Omrani A, Shameli A. Degradation kinetics of PET/PEN blend nanocomposites using differential isoconversional and differential master plot approaches. J Therm Anal Calorim. 2016;. doi:10.1007/s10973-015-5024-z.
19. Opfermann J. Kinetic analysis using multivariate non-linear regression: I. Basic concepts. J Therm Anal Calorim. 2000;60:641–58.
20. Lysenko EN, Surzhikov AP, Zhuravkov SP, Vlasov VA, Pustovalov AV, Yavorovsky NA. The oxidation kinetics study of ultrafine iron powders by thermogravimetric analysis. J Therm Anal Calorim. 2014;115:1447–52.
21. Perejón A, Sánchez-Jiménez PE, Criado JM, Pérez-Maqueda LA. Kinetic analysis of complex solid-state reactions. A new deconvolution procedure. J Phys Chem B. 2011;115:1780–91.
22. NETZSCH Thermokinetics Software Manual. Selb: NETZSCH-Geratebau GmbH; 2014 (Chapter 5.3.1).
23. Vyazovkin S. Isoconversional kinetics of thermally stimulated processes. Cham: Springer; 2015. p. 12.
24. Madorsky SL, Strauss S. Thermal degradation of polyethylene oxide and polypropylene oxide. J Polym Sci. 1959;36:183–94.
25. Liu L, Xu X. Polystyrene nanocomposites with improved combustion properties by using TMA-POSS and organic clay. J Therm Anal Calorim. 2016;. doi:10.1007/s10973-015-5181-0.
26. Triantou MI, Chatzigiannakis EM, Tarantili PA. Evaluation of thermal degradation mechanisms and their effect on the gross calorific value of ABS/PC/organoclay nanocomposites. J Therm Anal Calorim. 2015;119:337–47.